Supporting Materials

An unusual (3,4,4)-coordinated luminescent zinc(II) coordination polymer for selective detection of nitroaromatics, ferric and chromate ions: A versatile luminescent sensor

Ya-Qian Zhang,[a] Vladislav A. Blatov,[bc] Tian-Rui Zheng,[a] Chang-Hao Yang,[c] Lin-Lu Qian,[a] Ke Li,[a] Bao-Long Li*[a] and Bing Wu[a]

[a] State and Local Joint Engineering Laboratory for Functional Polymeric Materials, College of Chemistry, Chemical Engineering and Materials Science, Soochow University, Suzhou 215123, PR China. E-mail: libaolong@suda.edu.cn

[b] Samara Center for Theoretical Materials Science (SCTMS), Samara University, Ac. Pavlov St. 1, Samara 443011, Russia

[c] School of Materials Science and Engineering, Northwestern Polytechnical University, Xi'an, Shaanxi 710072, PR China

Table S1. Crystallographic data for **1**

Formula	$C_{54}H_{48}N_{18}O_{15}Zn_3$
Fw	1385.21
T/K	296(2)
Crystal system	Monoclinic
Space group	*C*2/c
a/Å	16.1735(12)
b/Å	12.0443(10)
c/Å	31.096(2)
α (°)	90
β (°)	100.881(2)
γ (°)	90
V /Å^3	5948.6(8)
F(000)	2832
Z	4
ρ_{calcd} (g cm^{-3})	1.547
μ(mm^{-1})	1.282
Reflections collected	84856
Unique reflections	6842 (R(int) = 0.1060)
Parameter	557
Goodness of fit	1.030
R_1 [I > 2σ(I)]	0.0771
wR_2 (all data)	0.2250

Table S2 Selected bond lengths and angles for **1** (Å and °).

Zn1-O1	1.989(4)	Zn1-O3A	1.969(4)
Zn1-N1	2.004(6)	Zn1-N7	1.989(6)
Zn2-O5B	2.211(5)	Zn2-O5C	2.211(5)
Zn2-O6B	2.217(5)	Zn2-O6C	2.217(5)
Zn2-N4	2.042(5)	Zn2-N4D	2.042(5)
O1-Zn1-O3A	97.93(16)	O1-Zn1-N1	117.8(2)
O1-Zn1-N7	108.8(2)	O3A-Zn1-N1	110.2(2)
O3A-Zn1-N7	107.4(2)	N1-Zn1-N7	113.3(2)
O5B-Zn2-O6B	57.87(18)	O5B-Zn2-O5C	90.6(3)
O5B-Zn2-O6C	105.2(2)	O5C-Zn2-O6B	105.15(19)
O5C-Zn2-O6C	57.87(18)	O6B-Zn2-O6C	157.8(3)
N4-Zn2-O5B	144.15(19)	N4-Zn2-O5C	97.59(19)
N4-Zn2-O6B	86.3(2)	N4-Zn2-O6C	108.7(2)
N4D-Zn2-O5B	97.59(19)	N4D-Zn2-O5C	144.15(19)

N4D-Zn2-O6B	108.7(2)	N4D-Zn2-O6C	86.3(2)
N4-Zn2-N4D	95.9(3)		

Symmetry transformations used to generate equivalent atoms: A 1/2+x, 1/2+y, +z; B 1-x, -y, 1-z; C +x, -y, 1/2+z; D 1-x, +y, 3/2-z.

Table S3 Average excited state lifetime (<τ>) values of **1** and in the presence of quenchers (λ_{ex} = 320 nm , λ_{em} = 410 nm).

CP	a1	a2	a3	τ1(ns)	τ2(ns)	τ3(ns)	<τ>(ns)
1	0.57	0.39	0.04	2.04	6.38	15.48	4.32
1+2 ppm TNP	0.30	0.55	0.15	1.17	3.33	10.37	3.75
1+0.05 mM Fe^{3+}	0.39	0.36	0.25	2.28	0.38	7.30	2.81
1+0.1mM $Cr_2O_7^{2-}$	0.40	0.44	0.16	1.32	3.94	10.14	3.90

Table S4 A comparison of the Stern-Volmer constant (K_{sv}), detection limit and medium used for Fe^{3+}, $Cr_2O_7^{2-}$, or CrO_4^{2-} detection for MOFs/CPs reported in references.

MOF/CP	Analyte	Solvent	Ksv	Detection Limit	Ref.
$\{[Tb_4(OH)_4(DSOA)_2(H_2O)_8]8H_2O\}_n$	Fe^{3+}	DMF	3.543×10^3 M^{-1}		S1
$[Cd(5\text{-}asba)(bimb)]_n$	Fe^{3+}	H_2O	1.78×10^4 M^{-1}	0.01875 mM	S2
$[(CH_3)_2NH_2][Tb(bptc)]xSolvents$	Fe^{3+}	EtOH		0.1801 mM	S3
$[H_2N(Me)_2][Eu_3(OH)(bpt)_3(H_2O)_3](DMF)_2(H_2O)_4$	Fe^{3+}	H_2O	3.2666×10^4 M^{-1}		S4
$[Zn5(hfipbb)_4(trz)_2(H_2O)_2]$	Fe^{3+}	H_2O		0.20 mM	S5
$[Me_2NH_2][Eu(CPA)_2(H_2O)_2]$	Fe^{3+}	H_2O	1.04111×10^4 M^{-1}	10^{-7} M	S6
$\{[Eu(L)(BPDC)_{0.5}(NO_3)]H_2O\}_n$	Fe^{3+}	DMF	5.16×10^4 M^{-1}		S7
$\{[Tb(L)(BPDC)_{0.5}(NO_3)]H_3O\}_n$	Fe^{3+}	DMF	4.30×10^4 M^{-1}		
$\{[Cd(L2)(HIP)]2H_2O\}_n$	Fe^{3+}	DMF	5.57×10^4 M^{-}	2.5 μM	S8

			^{1}		
$\{(Me_2NH_2)[Zn_2(L)(H_2O)]0.5DMF\}_n$	Fe^{3+}	DMF	7.83×10^{3} M^{-1}	1.44×10^{-5} M	S9
$\{[Eu(Hpzbc)_2(NO_3)]H_2O\}_n$	Fe^{3+}	EtOH		0.026 mM	S10
	$Cr_2O_7^{2-}$	EtOH		0.022 mM	
Eu_4L_3	Fe^{3+}	DMF	2.942×10^{3} M^{-1}	10^{-5} M	S11
	$Cr_2O_7^{2-}$	DMF	1.526×10^{3} M^{-1}	10^{-5} M	
$[Zn_6L_3(DMA)_4]5DMA$	Fe^{3+}	DMF		18 ppm	S12
$[Eu_3L_2(OH)(DMF)_{0.22}(H_2O)_{5.78}]$guest	Fe^{3+}	DMF		0.018 mM	S13
	$Cr_2O_7^{2-}$	DMF	6.63×10^{3} M^{-1}		
$\{[Cd(L)(BPDC)]2H_2O\}_n$	Fe^{3+}	H_2O	3.63×10^{4} M^{-1}	2.21×10^{-6} M	S14
	$Cr_2O_7^{2-}$	H_2O	6.4×10^{3} M^{-1}	3.76×10^{-5} M	
$\{[Cd(L)(SDBA)(H_2O)]0.5H_2O\}_n$	Fe^{3+}	H_2O	3.59×10^{4} M^{-1}	7.14×10^{-6} M	
	$Cr_2O_7^{2-}$	H_2O	4.97×10^{3} M^{-1}	4.86×10^{-5} M	
$[Tb(TBOT)(H_2O)](H_2O)_4(DMF)(NMP)_{0.5}$	Fe^{3+}	H_2O	5.51×10^{4} M^{-1}	0.13 mM	S15
	$Cr_2O_7^{2-}$	H_2O	1.37×10^{4} M^{-1}	0.14 mM	
$[Zn(IPA)(L)]_n$	$Cr_2O_7^{2-}$	H_2O	1.37×10^{3} M^{-1}	12.02 μM	S16
	CrO_4^{2-}	H_2O	1.00×10^{3} M^{-1}	18.33 μM	
$[Cd(IPA)(L)]_n$	$Cr_2O_7^{2-}$	H_2O	2.91×10^{3} M^{-1}	2.26 μM	
	CrO_4^{2-}	H_2O	1.30×10^{3} M^{-1}	2.52 μM	
$\{[Zn_3(mtrb)_3(btc)_2]\bullet3H_2O\}_n$	Fe^{3+}	H_2O	6.50×10^{3} M^{-1}	1.78 μM	This work
	$Cr_2O_7^{2-}$	H_2O	4.62×10^{3} M^{-1}	2.83 μM	
	CrO_4^{2-}	H_2O	2.77×10^{3} M^{-1}	4.52 μM	

References

S1 X.Y. Dong, R. Wang, J.Z. Wang, S.Q. Zang, T.C.W. Mak, *J. Mater. Chem. A*, 2015, **3**, 641.

S2 Y. J. Yang, M.J. Wang and K. L. Zhang, *J. Mater. Chem. C*, 2016, **4**, 11404.

S3 X. L. Zhao, D. Tian, Q. Gao, H. W. Sun, J. Wu and X. H. Bu, *Dalton Trans*., 2016, **45**, 1040.

S4 S. Xing, Q. Bing, L. Song, G. Li, J. Liu, Z. Shi, S. Feng, *Chem. Eur. J*., 2016, **22**, 16230.

S5 B. L. Hou, D. Tan, J. Liu, L. Z. Dong, S. L.Li, D. S. Li and Y. Q. Lan, *Inorg. Chem*., 2016, **55**, 10580.

S6 Y. P. Wu, G. W. Xu, W. W. Dong, J. Zhao, D. S. Li, J. Zhang and X. H. Bu, *Inorg. Chem*., 2017, **56**, 1402.

S7 W. Yan, C. L. Zhang, S. G. Chen, L. J. Han and H. G. Zheng, *ACS Appl. Mater. Interface*, 2017, **9**, 1629.

S8 X. Zhang, Z. J. Wang, S. G. Chen, Z. Z. Shi，J. X. Chen and H.G. Zheng, *Dalton Trans*., 2017, **46**, 2332.

S9 J. Wang, X. R. Wu, J. Q. Liu, B. H. Li, A. Singh, A. Kumar and S. R. Batten, *CrystEngComm*, 2017, **19**, 3519.

S10 G. P. Li, G. Liu, Y. Z. Li, L. Hou, Y. Y.Wang and Z. Zhu, *Inorg. Chem*., 2016, **55**, 3952;

S11 W. Liu, X. Huang, C. Xu, C. Y. Chen, L. Z. Yang, W. Dou, W. M. Chen, H. Yang and W. S. Liu, *Chem. Eur. J*., 2016, **22**, 18769.

S12 B. H. Li, J. Wu, J. Q. Liu, C. Y. Gu, J. W. Xu, M. M. Luo, R. Yadav, A. Kumar and S. R. Batten, *ChemPlusChem*, 2016, **81**, 885.

S13 J. Q. Liu, G. P. Li, W. C. Liu, Q. L. Li, B. H. Li, R. W. Gable, L. Hou and S. R. Batten, *ChemPlusChem*, 2016, **81**, 1299.

S14 S. G. Chen, Z. Z. Shi, L. Qin, H. L. Jia and H. G. Zheng, *Cryst. Growth Des*., 2017, **17**, 67.

S15 M. Chen, W. M. Xu, J. Y. Tian, H. Cui, J. X. Zhang, C. S. Liu, M. Du, *J. Mater. Chem. C*, 2017, **5**, 2015.

S16 B. Parmar, Y. Rachuri, K. K. Bisht, R. Laiya and E. Suresh, *Inorg. Chem*., 2017, **56**, 2627.

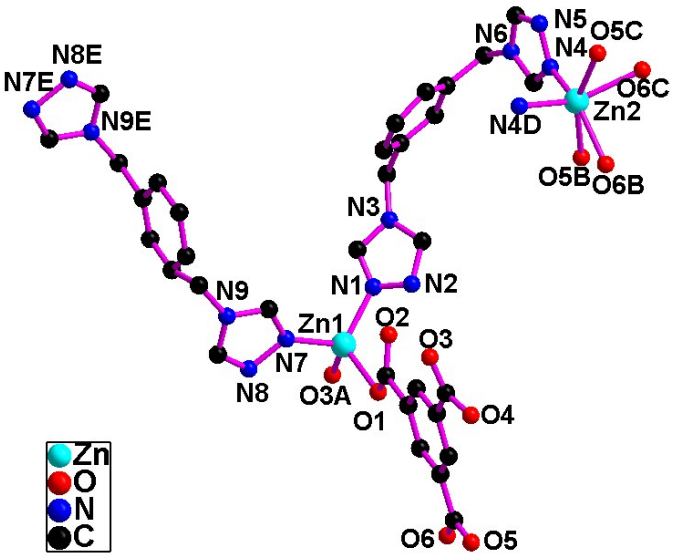

Fig. S1 (a) The coordination environment of Zn(II) atoms in **1**.

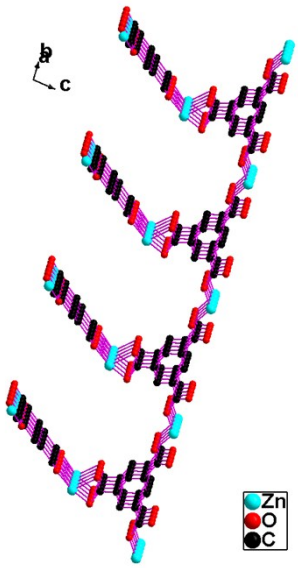

Fig. S1 (b) Side viewing the $[Zn_3(btc)_2]_n$ 2D network in **1**.

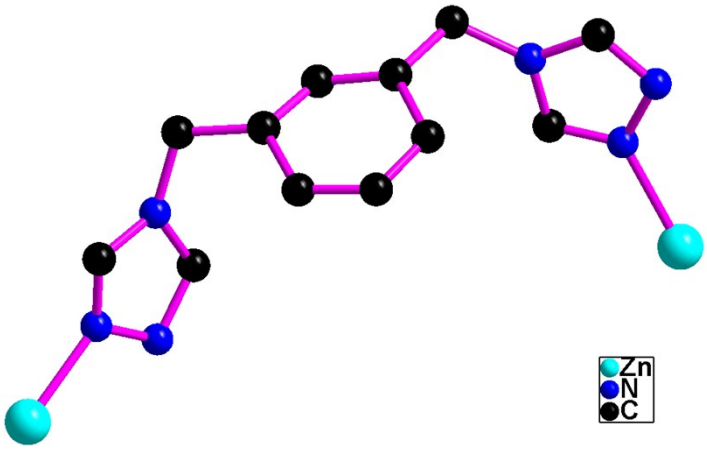

Fig. S1 (c) The coordination mode of mtrb ligand in **1**.

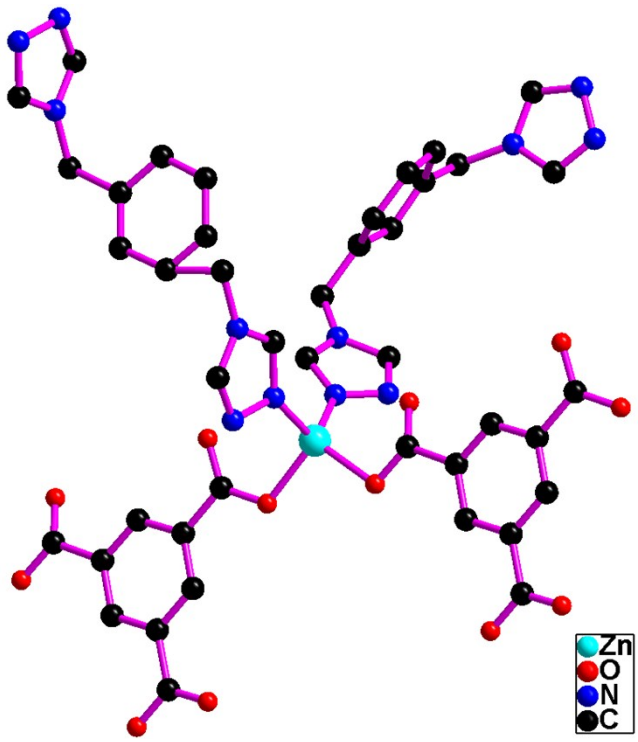

Fig. S1 (d) The 4-coordinated Zn(II) atom in **1**.

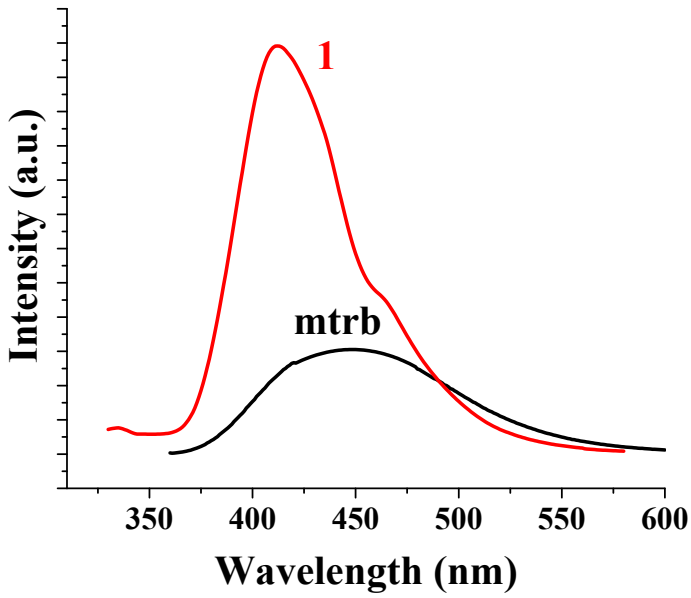

Fig. S2 Solid-state emission spectra of **1** and the free mtrb ligand at room temperature.

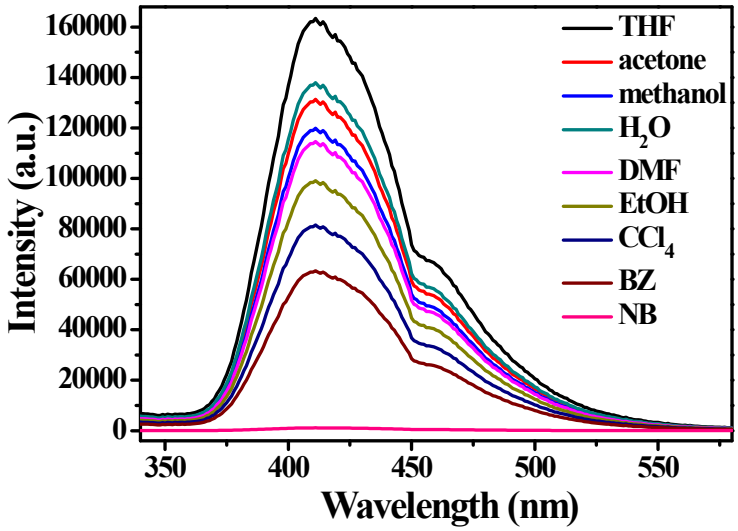

Fig. S3 Emission spectra of **1** in different solvents (excited at 320 nm).

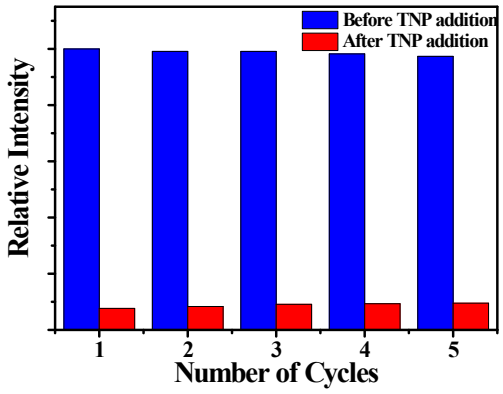

Fig. S4 Reproducibility of the quenching ability of **1** in the detection of TNP.

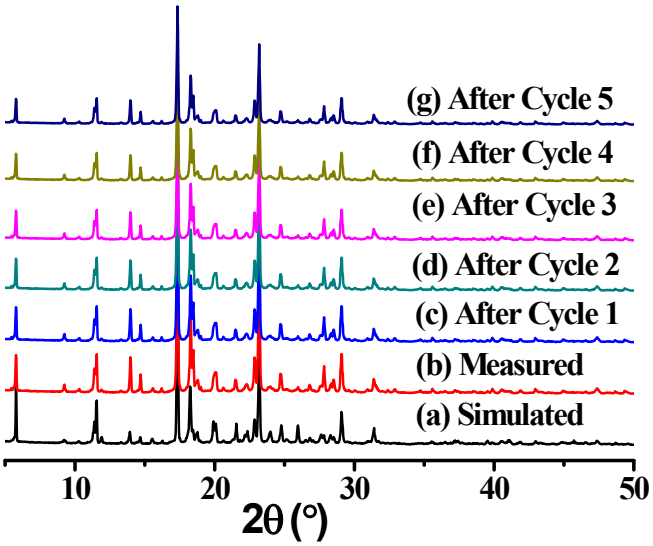

Fig. S5 PXRD patterns of the simulated and measured of **1**, cycle 1 – 5 after detection of TNP.

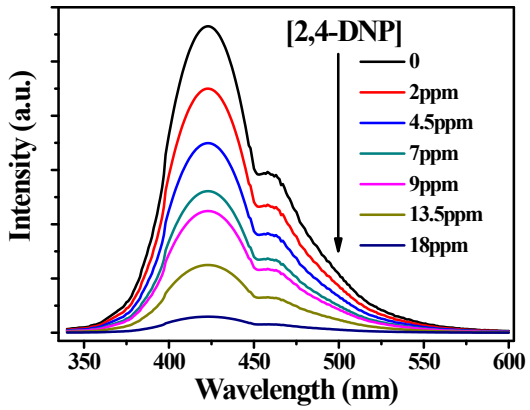

Fig. S6 (a) Emission spectra of **1** dispersed in MeOH in the presence of various amounts of 2,4-DNP.

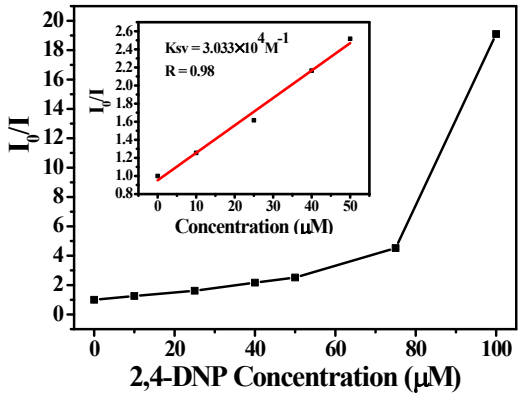

Fig. S6 (b) The relationship between I_0/I and different concentration of 2,4-DNP. Insert: linear plot of I_0/I at low concentration of 2,4-DNP.

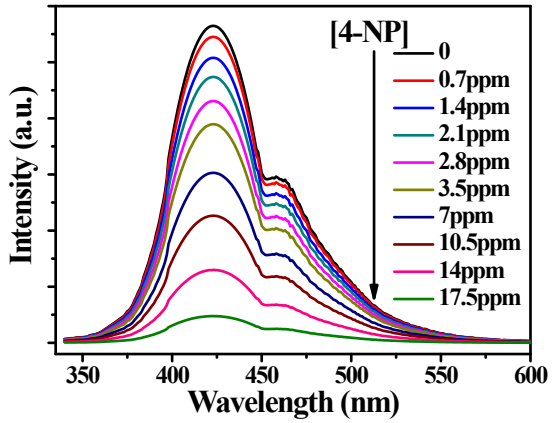

Fig. S7 (a) Emission spectra of **1** dispersed in MeOH in the presence of various amounts of 4-NP.

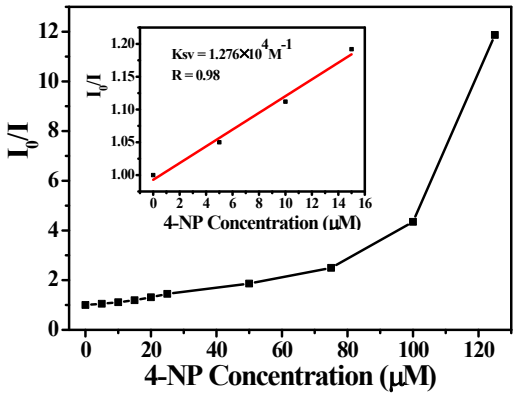

Fig. S7 (b) The relationship between I_0/I and different concentration of 4-NP. Insert: linear plot of I_0/I at low concentration of 4-NP.

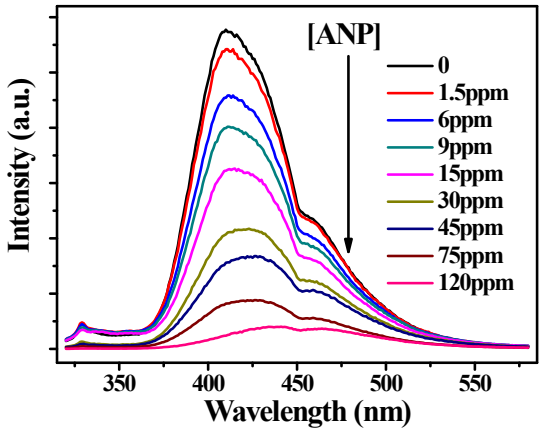

Fig. S8 (a) Emission spectra of **1** dispersed in MeOH in the presence of various amounts of ANP.

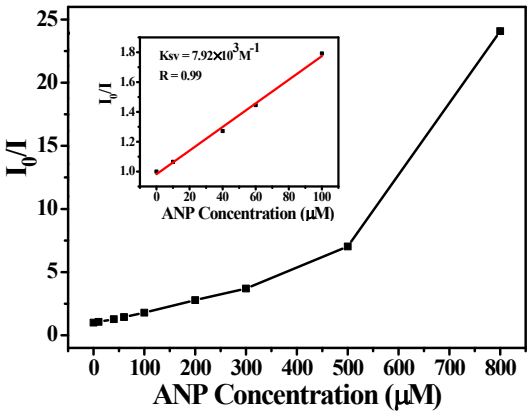

Fig. S8 (b) The relationship between I_0/I and different concentration of ANP. Insert: linear plot of I_0/I at low concentration of ANP.

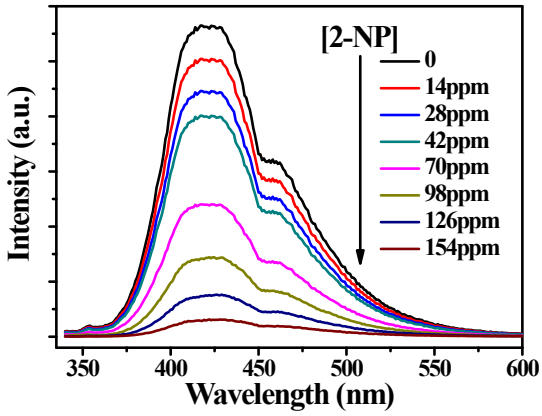

Fig. S9 (a) Emission spectra of **1** dispersed in MeOH in the presence of various amounts of 2-NP.

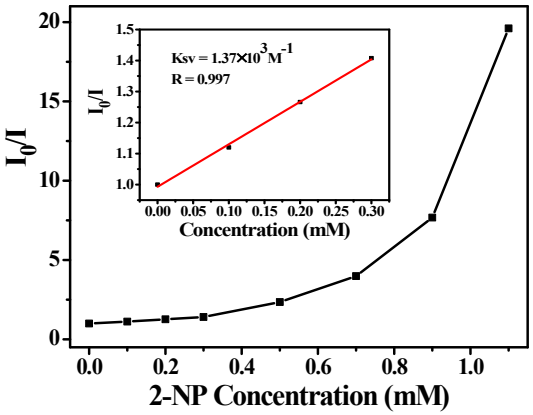

Fig. S9 (b) The relationship between I_0/I and different concentration of 2-NP. Insert: linear plot of I_0/I at low concentration of 2-NP.

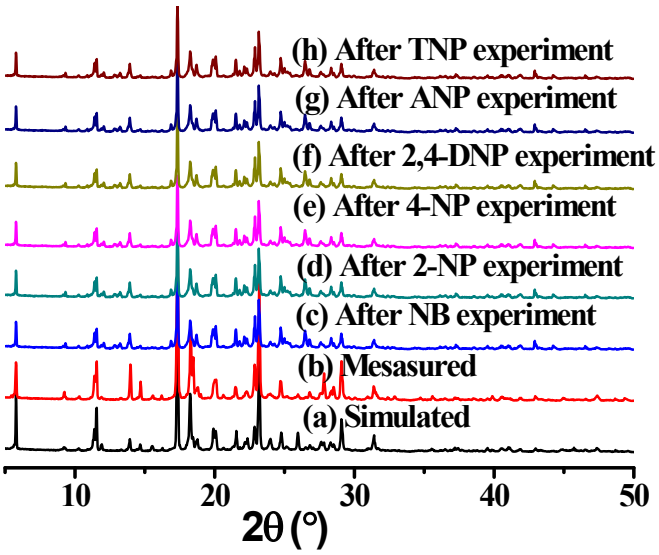

Fig. S10 PXRD patterns of the measured, simulated and measured of **1**, after detection of nitroaromatics analytes in MeOH solutions.

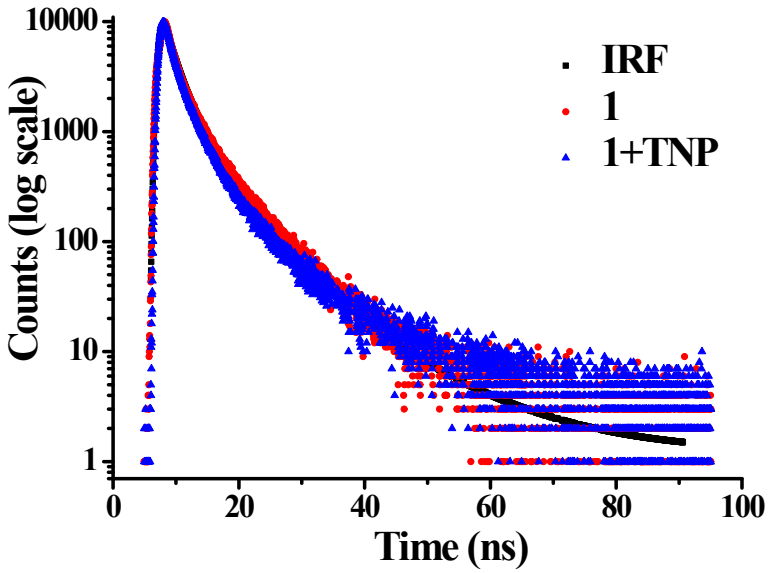

Fig. S11 Fluorescence decay of **1** and **1** in the presence of 2 ppm TNP (IRF = Instrument Response Function) (λ_{ex} = 320 nm , λ_{em} = 410 nm).

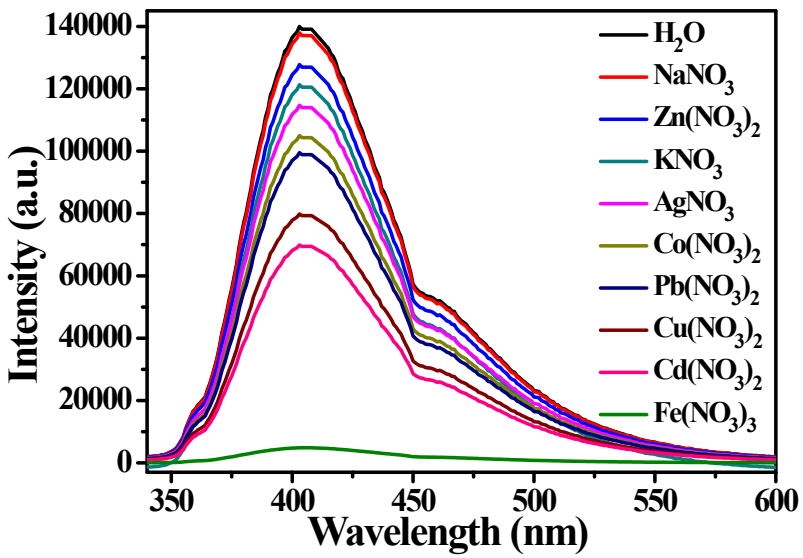

Fig. S12 Emission spectra of **1** dispersed in aqueous solution in the presence of different metal cations (3.0 mM).

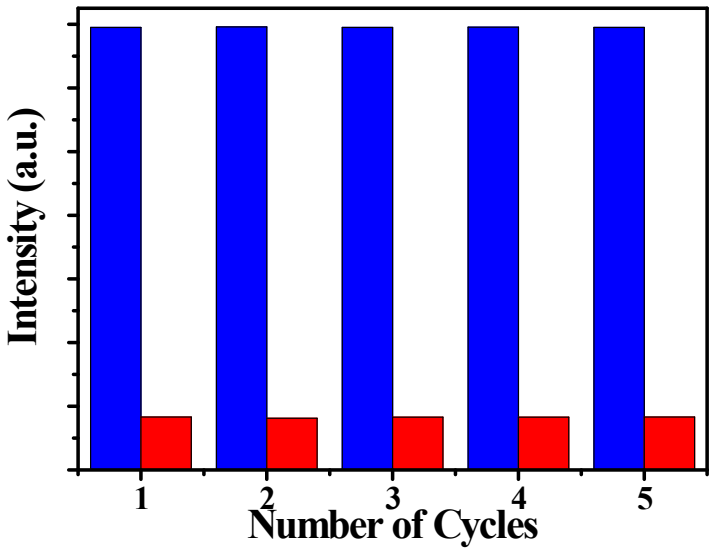

Fig. S13 Reproducibility of the quenching ability of **1** in the detection of Fe^{3+}.

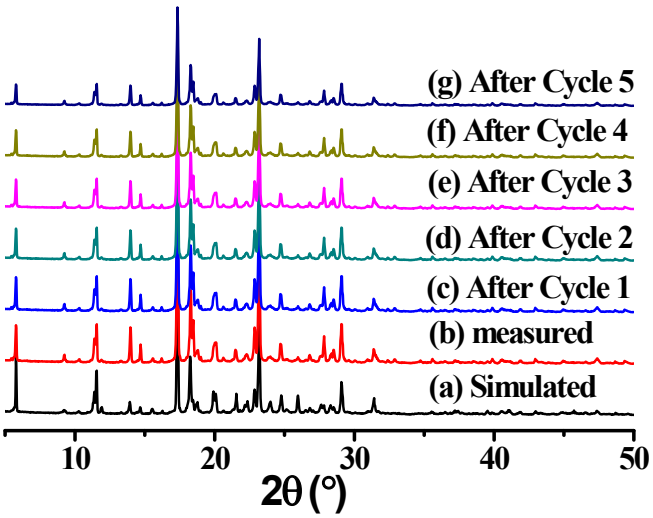

Fig. S14 PXRD patterns of the simulated and measured of **1**, cycle 1 – 5 after detection of Fe^{3+}.

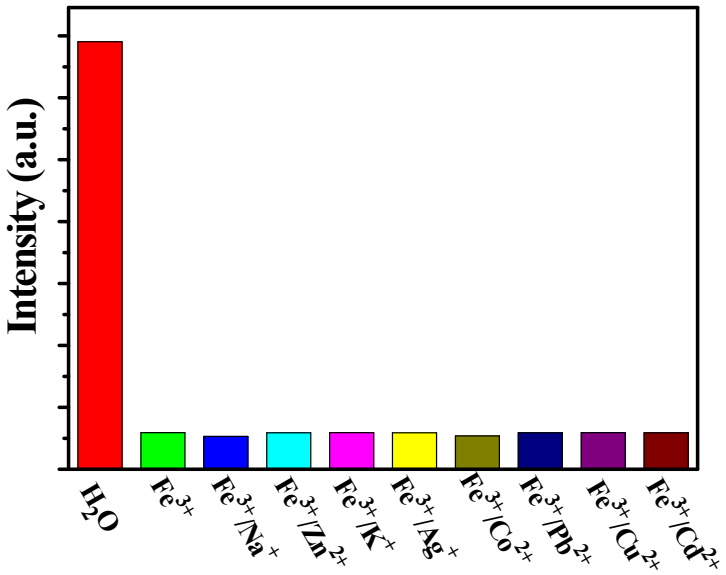

Fig. S15 Emission intensity of **1** dispersed in the aqueous solution of Fe^{3+} (1.0 mM) in the presence of different metal cations (1.0 mM).

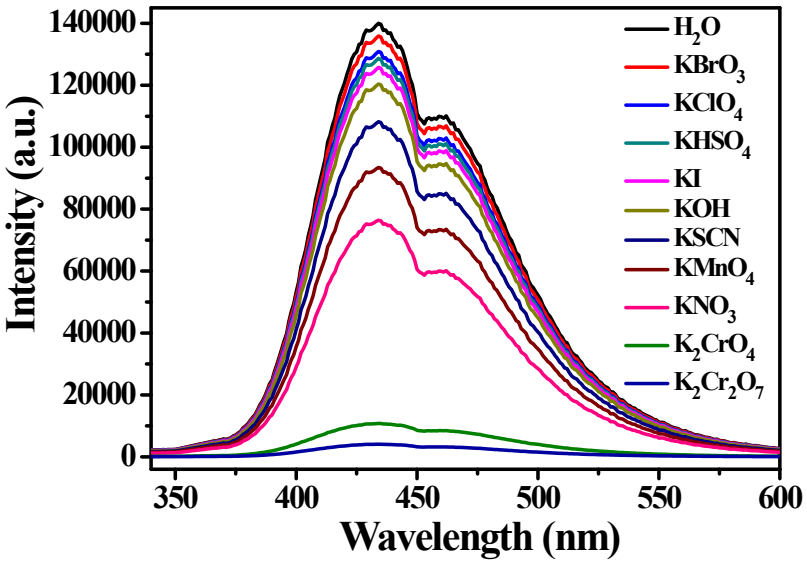

Fig. S16 Emission spectra of **1** dispersed in aqueous solution in the presence of different anions (1.0 mM).

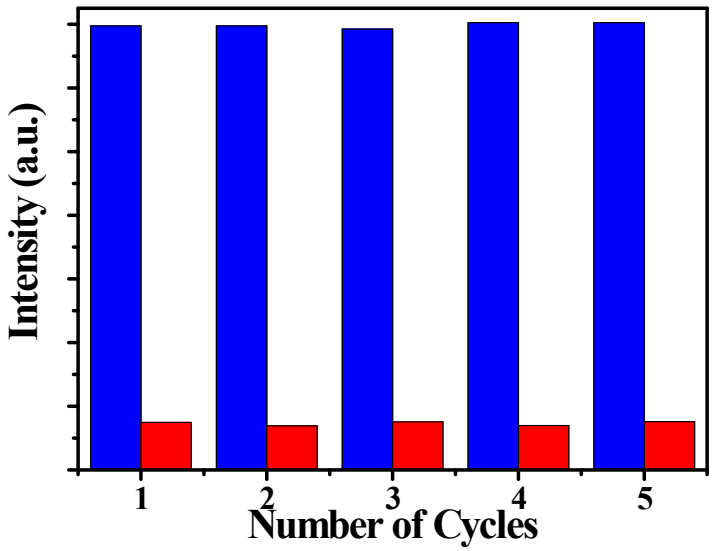

Fig. S17 Reproducibility of the quenching ability of **1** in the detection of $Cr_2O_7^{2-}$.

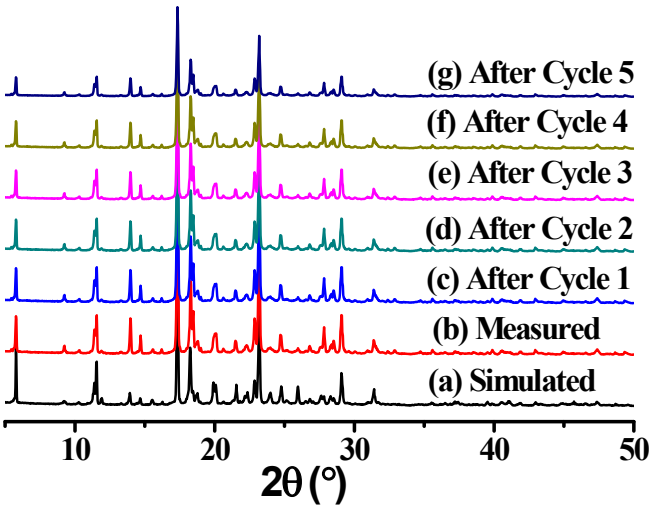

Fig. S18 PXRD patterns of the simulated and measured of **1**, cycle 1 – 5 after detection of $Cr_2O_7^{2-}$.

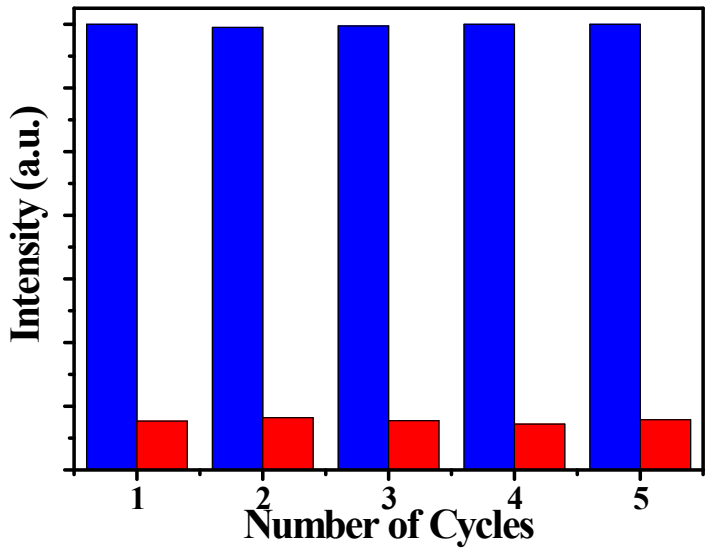

Fig. S19 Reproducibility of the quenching ability of **1** in the detection of CrO_4^{2-}.

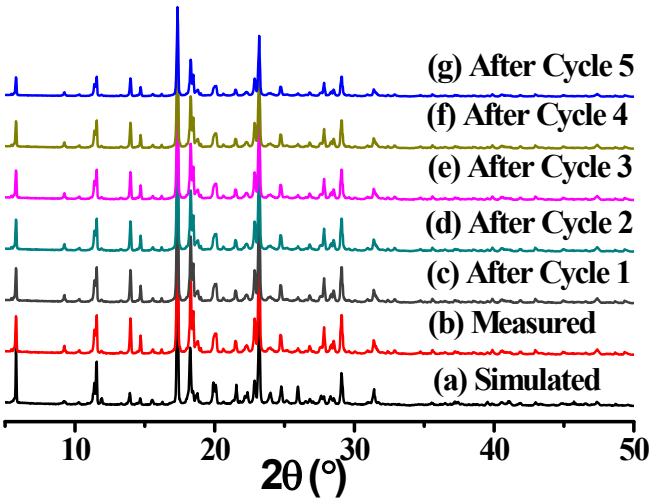

Fig. S20 PXRD patterns of the simulated and measured of **1**, cycle 1 – 5 after detection of CrO_4^{2-}.

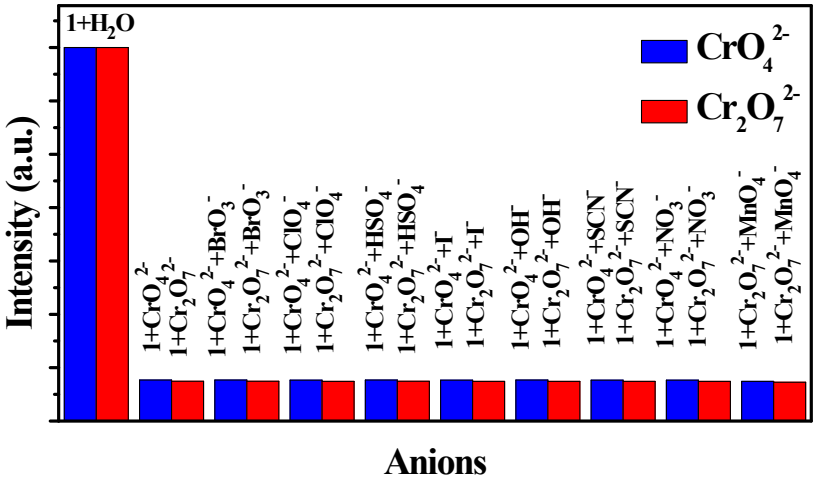

Fig. S21 Emission intensity of **1** dispersed in the aqueous solution of $Cr_2O_7^{2-}$ (0.9 mM), or CrO_4^{2-} (1.5 mM) in the presence of different ions (3.0 mM).

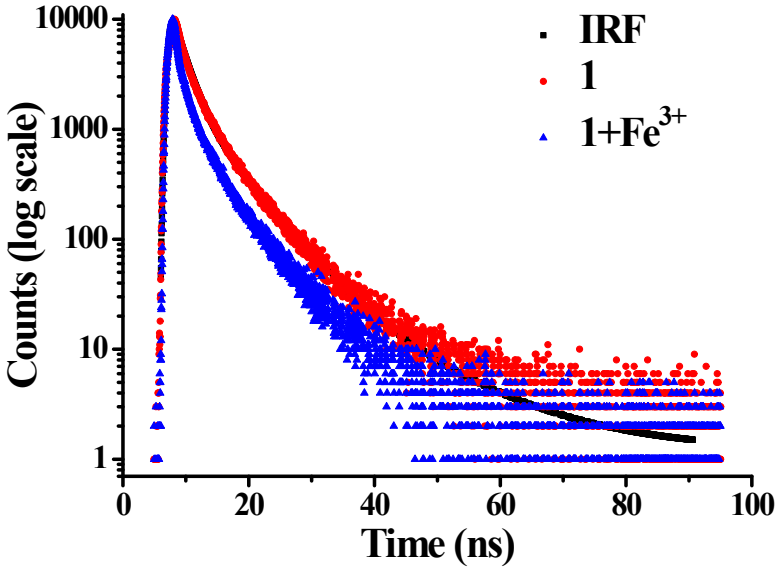

Fig. S22 Fluorescence decay of **1** and **1** in the presence of 0.05 mM Fe^{3+} (IRF = Instrument Response Function) (λ_{ex} = 320 nm , λ_{em} = 410 nm).

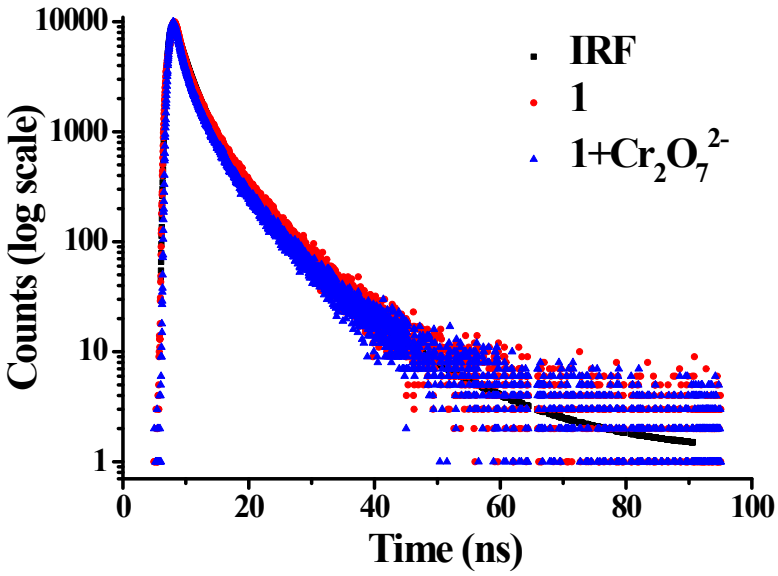

Fig. S23 Fluorescence decay of **1** and **1** in the presence of 0.1 mM $Cr_2O_7^{2-}$ (IRF = Instrument Response Function) (λ_{ex} = 320 nm , λ_{em} = 410 nm).

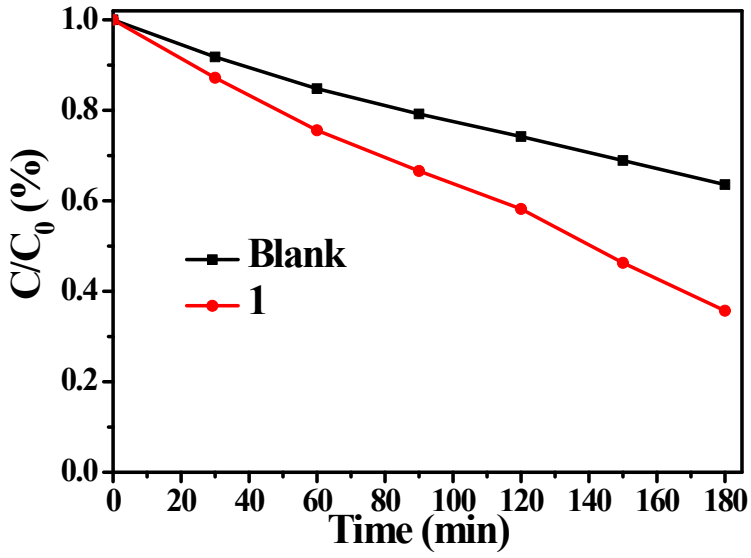

Fig. S24 Photocatalytic degradation efficiencies of the MB solution under UV light irradiation using catalyst **1** and blank experiment (only H_2O_2).